

Three-dimensional Finite Difference-Time Domain Solution of Dirac Equation

Neven Simicevic §

Center for Applied Physics Studies, Louisiana Tech University, Ruston, LA 71272, USA

Abstract. The Dirac equation is solved using three-dimensional Finite Difference-Time Domain (FDTD) method. *Zitterbewegung* and the dynamics of a well-localized electron are used as examples of FDTD application to the case of free electrons.

PACS numbers: 03.65.Pm, 02.60.-x, 02.60.Lj

§ Correspondence should be addressed to Louisiana Tech University, PO Box 10348, Ruston, LA 71272, Tel: +1.318.257.3591, Fax: +1.318.257.4228, E-mail: neven@phys.latech.edu

In this letter, for the first time, full three-dimensional FDTD method to solve the Dirac equation is described. The Finite Difference-Time Domain (FDTD) method is a fast growing numerical method originally introduced by Kane Yee [1] to solve Maxwell's equations. In the last two decades the method was intensively developed primarily in the field of electrodynamics [2, 3, 4, 5], but was, at a much lower scale, also extended to other fields of applications such as acoustics and elastodynamics. When applied to solving Maxwell's equations, the FDTD method is relatively simple and numerically robust, has almost no limit in the description of geometrical and dispersive properties of the material, and is appropriate for the computer technology of today. As an example, we have applied the FDTD method to calculate the exposure of complex biological tissues to non-ionizing ultra-wide band (UWB) radiation using high-resolution description of the geometry and realistic physical properties of exposed material over a broad frequency range [6, 7].

In the case of electrodynamics, the FDTD method was able to solve problems with complexity that was far beyond allowing analytical solutions and was fundamental to the advancement of electrical engineering [5]. In the same sense, we expect that the application of FDTD method in quantum mechanics, in this particular case for the solution of the Dirac equation, will become a stepping stone for the advancement of modern physics.

Similarities between Maxwell's equations and the Dirac equation are obvious if the Dirac equation is written, in a standard notation, as a system of two first-order equations [8]

$$\begin{aligned} [i\hbar\sigma \cdot \nabla - i\frac{\hbar}{c}\frac{\partial}{\partial t}]\Phi^{(L)} &= -mc\Phi^{(R)}, \\ [-i\hbar\sigma \cdot \nabla - i\frac{\hbar}{c}\frac{\partial}{\partial t}]\Phi^{(R)} &= -mc\Phi^{(L)}. \end{aligned} \quad (1)$$

Two component wave functions $\Phi^{(R)}$ and $\Phi^{(L)}$ couple in these equations as the electric \vec{E} and magnetic \vec{B} fields couple in Maxwell's equations [8].

While the FDTD scheme can be applied to Eq. (1), it is applied here to the form originally written by Dirac. In the case when the electromagnetic field described by the four-potential $A^\mu = \{A_0(x), \vec{A}(x)\}$ is minimally coupled to the particle, the Dirac equation can be written as

$$i\hbar\frac{\partial\Psi}{\partial t} = (H_{free} + H_{int})\Psi, \quad (2)$$

where

$$H_{free} = -i\hbar\alpha \cdot \nabla + \beta mc^2, \quad (3)$$

$$H_{int} = -e\alpha \cdot \vec{A} + eA_0, \quad (4)$$

and

$$\Psi(x) = \begin{pmatrix} \Psi_1(x) \\ \Psi_2(x) \\ \Psi_3(x) \\ \Psi_4(x) \end{pmatrix}. \quad (5)$$

Matrices α and β are expressed using 2×2 Pauli matrices σ 's and the 2×2 unit matrix I [8].

The FDTD schematics to solve Eq. (2) follows Yee's leapfrog algorithm [1]. Space and time are discretized using uniform rectangular lattices of size Δx , Δy and Δz , and uniform time increment Δt . Any function $f(x, y, z, t)$ becomes $f(i\Delta x, j\Delta y, k\Delta z, n\Delta t) \equiv f_{i,j,k}^n$, where i, j, k , and n are integers. Partial derivatives are expressed numerically with second order accuracy as follows:

- space derivative in the x-direction at fixed time $n\Delta t$

$$\frac{\partial f_{i,j,k}^n}{\partial x} \approx \frac{f_{i+1,j,k}^n - f_{i-1,j,k}^n}{2\Delta x}. \quad (6)$$

Analogously for derivatives in y- and z-directions.

- time derivative at fixed position $f(i\Delta x, j\Delta y, k\Delta z)$

$$\frac{\partial f_{i,j,k}^n}{\partial t} \approx \frac{f_{i,j,k}^{n+1/2} - f_{i,j,k}^{n-1/2}}{\Delta t} \quad (7)$$

In the case of electrodynamics the electric field \vec{E} at the time $n - 1/2$ is used to calculate magnetic field \vec{H} at the time n , which in turn is used to calculate the electric field \vec{E} at the time $n + 1/2$, and so on. In the case of the Dirac equation the wave functions Ψ_1 and Ψ_2 at the time $n - 1/2$ are used to calculate the wave functions Ψ_3 and Ψ_4 at the time n , which are then used to calculate the wave functions Ψ_1 and Ψ_2 at the time $n + 1/2$, and so on. The same numerical requirements as in the case of electrodynamics were followed. Numerical dispersion and stability criteria developed for the electromagnetic case [5] were analogously applied to solving the Dirac equation. The Courant stability condition was imposed to the time step Δt

$$\Delta t \leq \frac{1}{c\sqrt{(\Delta x)^{-2} + (\Delta y)^{-2} + (\Delta z)^{-2}}}, \quad (8)$$

and, as a consequence of the Nyquist sampling limit [3], the rectangular lattices size

$$\Delta x \sim \Delta y \sim \Delta z < \lambda/2. \quad (9)$$

λ is the wavelength of the plane-wave solution. In practical applications the size of the lattice is typically between $\lambda/10$ and $\lambda/20$. In the case of *Zitterbewegung*, the spatial oscillation of the wave packet due to an interference between the positive and negative energy components [8], one more condition was imposed to the lattice sizes

$$\Delta x \sim \Delta y \sim \Delta z < \frac{\hbar}{2mc}. \quad (10)$$

Boundary conditions appropriate for extending the finite computational domain to infinity are applied by extrapolations similar to Liao extrapolation [9]. The physical solutions inside the computational domain are extended outside the domain using Newton's interpolation polynomials [5].

The updating difference equation for Ψ_1 was obtained by solving the algebra of Eq. (2), applying Eq. (6) and (7), and simplifying using $\Delta x = \Delta y = \Delta z$

$$\begin{aligned}
 \Psi_1^{n+1/2}(I, J, K) &= \frac{2 - C^n(I, J, K)}{C^n(I, J, K)} \Psi_1^{n-1/2}(I, J, K) \\
 &- \frac{c\Delta t}{2\Delta x C^n(I, J, K)} [\Psi_3^n(I, J, K + 1) - \Psi_3^n(I, J, K - 1) \\
 &+ \Psi_4^n(I + 1, J, K) - \Psi_4^n(I - 1, J, K) - i(\Psi_4^n(I, J + 1, K) \\
 &- \Psi_4^n(I, J - 1, K))] + i \frac{e\Delta t}{\hbar C^n(I, J, K)} [A_1^n(I, J, K) \Psi_4^n(I, J, K) \\
 &- iA_2^n(I, J, K) \Psi_4^n(I, J, K) + A_3^n(I, J, K) \Psi_3^n(I, J, K)], \quad (11)
 \end{aligned}$$

where $C^n(I, J, K) = 1 + i \frac{\Delta t}{2\hbar} [mc^2 + eA_0^n(I, J, K)]$. Updating equations for Ψ_2 , Ψ_3 , and Ψ_4 were constructed in a similar way. The dynamics of a Dirac electron can be now studied in an environment described by any four-potential A^μ regardless of its complexity and time dependency. As a result of limited space in this letter only few cases were chosen.

Following the analytical solution of K. Huang [10], we studied the model-independent motion of a free Dirac electron acquired from the Dirac equation itself. It is important to stress that, as a consequence of the Dirac equation being linear in $\partial/\partial t$, the entire dynamics of the electron is defined by its initial wave function only. As in the case of Maxwell's equations, no initial velocity needs to be specified. The dynamics of the wave packet studied here was defined by its initial wave function

$$\Psi(\vec{x}, 0) = N \sqrt{\frac{E + mc^2}{2E}} \begin{pmatrix} 1 \\ 0 \\ \frac{p_3 c}{E + mc^2} \\ \frac{(p_1 - ip_2)c}{E + mc^2} \end{pmatrix} e^{-\frac{\vec{x} \cdot \vec{x}}{4x_0^2} + \frac{i\vec{p} \cdot \vec{x}}{\hbar}}, \quad (12)$$

where N is a normalizing constant, $N = [(2\pi)^{3/2} x_0^3]^{-1/2}$. Eq. (12) represents a wave packet whose initial probability distribution is of a normalized Gaussian shape with its size defined by the constant x_0 . Its spin is pointed along the z-axis and its motion is defined by the values of p_1, p_2 , and p_3 . In the "single particle interpretation" of the Dirac equation, if we choose $p_2 = p_3 = 0$ and $p_1 \neq 0$ the wave packet should move in +x-direction. This is not the case. Because of the localization of the wave packet and limitation of the direction of the spin, the initial condition in Eq. (12) contains also a significant negative energy component moving in the -x-direction [10]. Dynamics of this wave packet, for $p_1 = 18.75 \text{ MeV}/c$ and $x_0 = 10^{-11} \text{ m}$, is shown in Fig. 1.

Another aspect of the motion of the Dirac electron consists of *Zitterbewegung*, rapid oscillatory motion around a uniform rectilinear motion attributed to interference between positive and negative energy states [8]. The FDTD, being a time-domain method, is an excellent tool to study the properties of *Zitterbewegung*. Few results are presented here. Fig. 2 shows the time dependence of the position of the center of probability in the x-y plane of the fraction of our wave-packet moving in the -x-direction at the beginning of motion. The amplitude of the motion in this particular

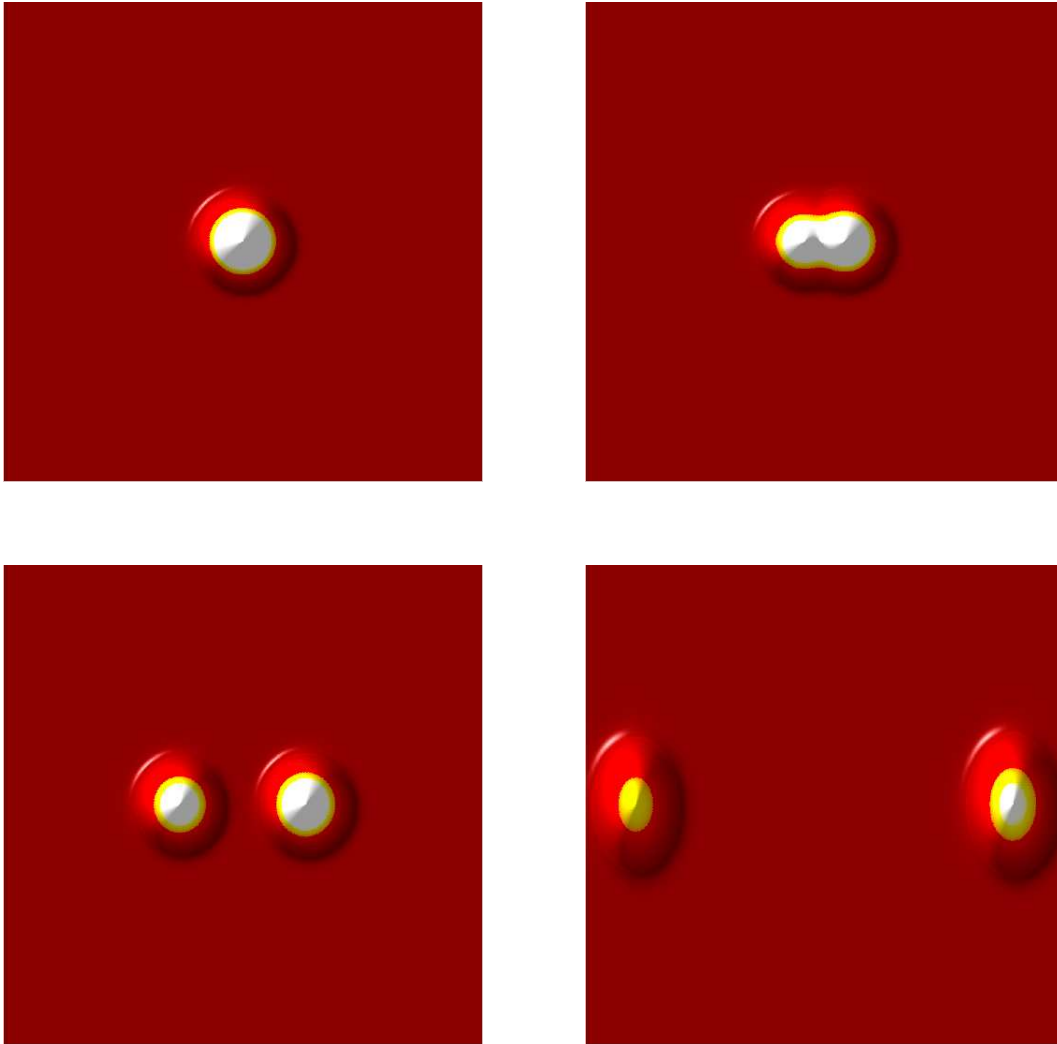


Figure 1. Top view of the four different stages of motion of the wave packet initialized by Eq. (12) in the x-y plane. The initial wave packet splits in two, moving in both the positive and negative x-directions, corresponding to positive and negative energy solutions. It is important to notice details of electron dynamics through changing of the shape of the wave packets into elliptical as a result of relativistic suppression of the wave packet spreading in the direction of motion for a massive particle [11]. The full animations can be accessed on-line [12].

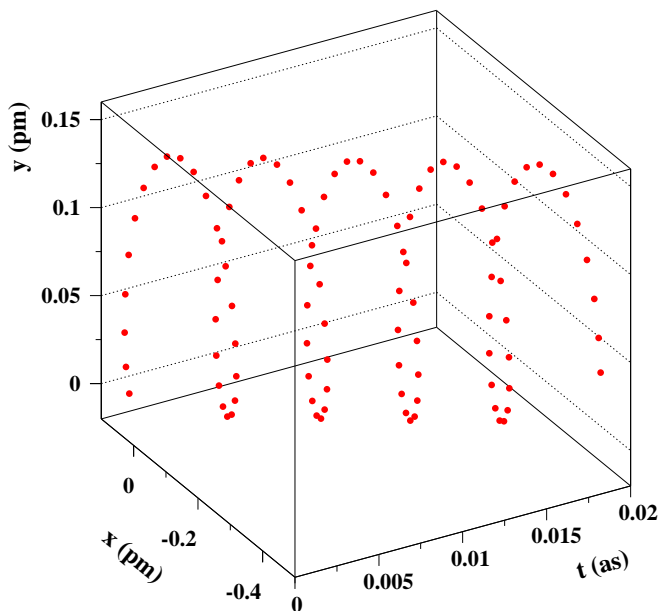


Figure 2. Time dependence of the position of the center of probability of the fraction of the wave-packet defined by Eq. (12) moving in the $-x$ -direction at the beginning of motion.

case is 1.45×10^{-11} cm, of the order of \hbar/mc as predicted [8]. Fig. 3 shows the x -position of the fraction of the wave-packet moving in the $+x$ -direction. *Zitterbewegung* exists at the beginning of the motion, at the time when positive- and negative-energy components of the wave packets shown in Fig. 1 overlap. It is absent as the wave packets separate. Lack of space in this letter prevents discussion of *Zitterbewegung*-related violent and rapid oscillations of the velocity of the electron.

The frequency of *Zitterbewegung* can easily be obtained. Fitting the probability function, as shown in Fig. 4, we found the angular frequency of $\omega = (1.582 \pm 0.009) \times 10^{21}$ Hz for $p_1 = 18.75$ MeV/c and $\omega = (1.525 \pm 0.009) \times 10^{21}$ Hz for $p_1 = 187.5$ eV/c. It is in agreement with expected angular frequency of $\sim 2mc^2/\hbar$ and shows little momentum dependence.

Finally, we discuss briefly the well-localized state described, for example, by

$$\Psi(\vec{x}, 0) = N \begin{pmatrix} 1 \\ 0 \\ 0 \\ 0 \end{pmatrix} e^{-\frac{\vec{x} \cdot \vec{x}}{4x_0^2}}. \quad (13)$$

Snapshots of the dynamics of the probability densities of this state for $x_0 = 10^{-14}$ m, simulating localization in a volume of the size of the atomic nucleus, are shown in Fig. 5.

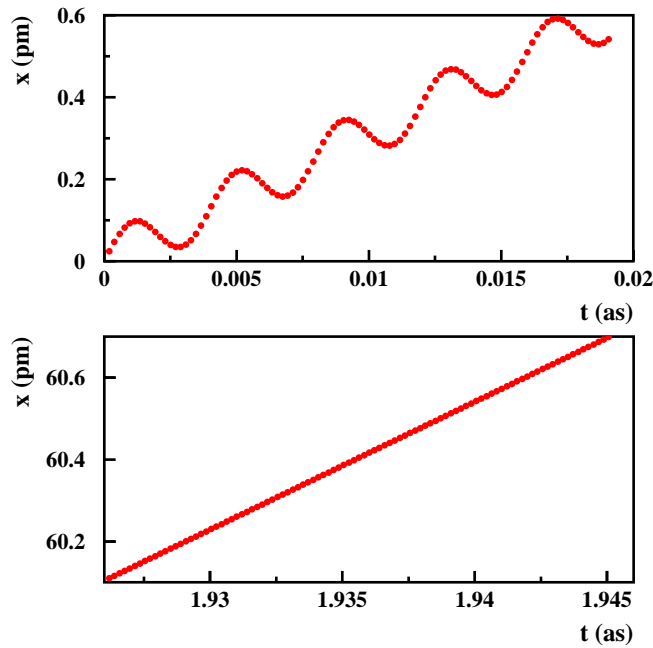


Figure 3. X-position of the fraction of the wave-packet shown in Fig. 1 moving in the +x-direction. The *Zitterbewegung* which exists at the beginning of the motion (top) is absent after positive- and negative-energy components separate (bottom).

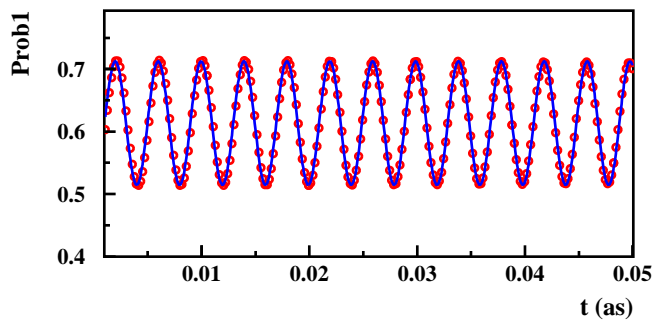


Figure 4. Fit of the probability function used to determine the frequency of *Zitterbewegung*.

FDTD computation shows that the angular distribution of probability density $|\Psi_1|^2$ is determined by spherical harmonic Y_{00} , the density $|\Psi_2|^2$ is 0, the angular distribution of $|\Psi_3|^2$ is determined by spherical harmonic Y_{10} , and $|\Psi_4|^2$ by Y_{11} . The radial dependence of $|\Psi_1|^2$ is determined by the spherical Bessel functions j_0 , and $|\Psi_3|^2$ and $|\Psi_4|^2$ by j_1 . The time dependent behavior of the total probabilities is shown in Fig. 6. After the first shock, attributed to *Zitterbewegung* resulting from the initial condition, total probabilities acquire the values of $Prob1 : Prob2 : Prob3 : Prob4 = 1/2 : 0 : 1/6 : 1/3$. The ratios of those probabilities result from the Clebsch-Gordan coefficients which are part of the relation between spherical harmonic spinors Ω_{jlm} and spherical harmonics

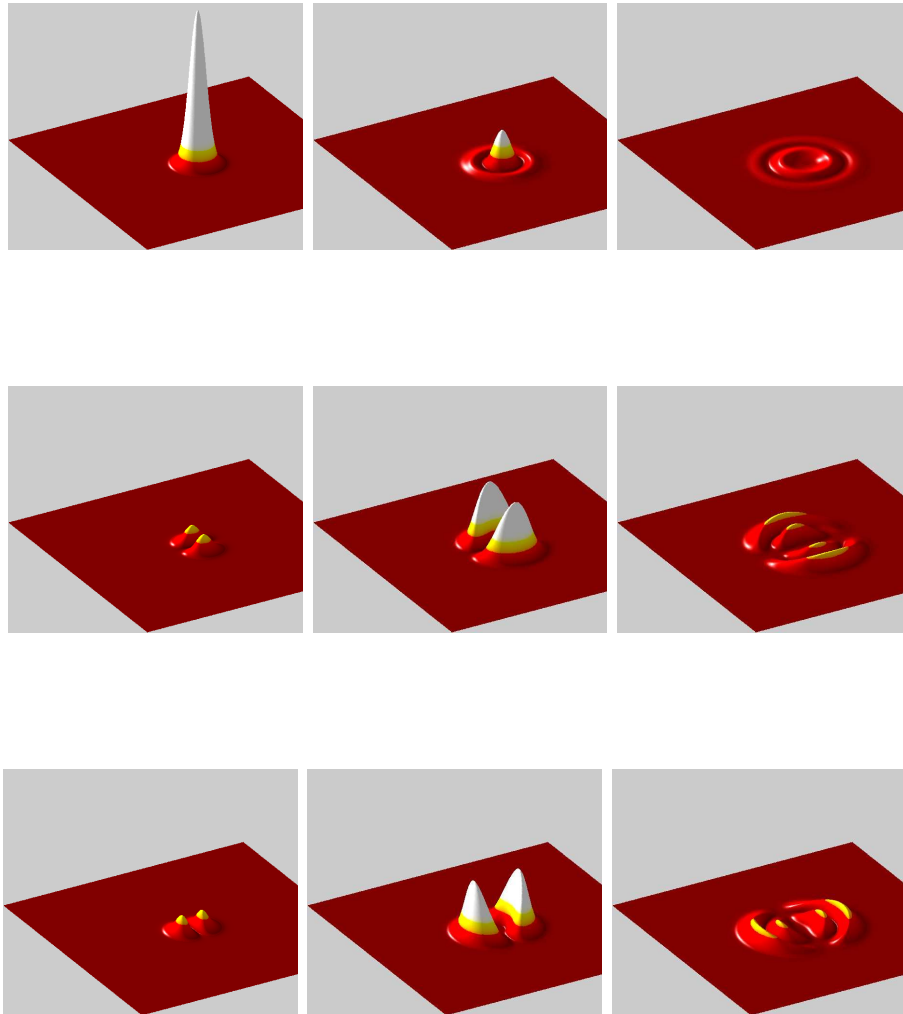


Figure 5. Three different stages of motion of the wave packet in the x - z plane initialized by Eq. (13). Top-row is probability density $|\Psi_1|^2$, mid-row $|\Psi_3|^2$, and bottom-row $|\Psi_4|^2$. The associated animations can be accessed on-line [12].

Y_{lm} [13, 14]. (Those ratios persist for more localized states, for example for $x_0 = 10^{-15} m$, but, as expected, change for less localized states.) The angular and radial distribution of the probability densities and the values of the total probability determined by the FDTD method show that the state with initially localized position and spin, corrects its state in a very short time (Fig. 6) and behaves as a spherical wave.

To conclude, for the first time full three-dimensional Finite Difference Time Domain (FDTD) method was developed to solve the Dirac equation. In this paper the method was applied to the dynamics of a free Dirac electron, comparing some of the results to the analytical solutions. Forthcoming work will study the dynamics of the Dirac electron

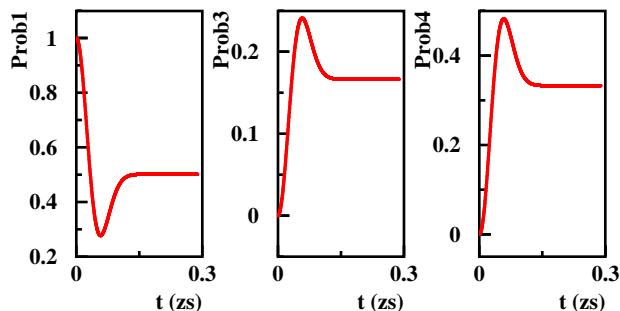


Figure 6. Time dependence of the total probabilities of the wave packet defined by Eq. (13).

in potential fields. The impact of FDTD method in electrodynamics warranted that the first chapter of the book by A. Taflove and S. C. Hagnes [5] be titled “Electrodynamics Entering the 21st Century”. We hope that the FDTD method will have the same impact on better understanding, advancing, and applying modern physics.

I would like to thank B. Ramu Ramachandran, Lee Sawyer and Steve Wells for useful comments. Also, the use of the high-performance computing resources provided by Louisiana Optical Network Initiative (LONI; www.loni.org) is gratefully acknowledged.

References

- [1] K. S. Yee, *IEEE Trans. Antennas Propagat.* **AP-14**, 302 (1966).
- [2] M. N. O. Sadiku, *Numerical Techniques in Electromagnetics* (CRC Press LLC, Boca Raton, FL, 1992).
- [3] K. Kunz and R. Luebbers, *The Finite Difference Time Domain Method for Electromagnetics*(CRC Press LLC, Boca Raton, FL, 1993).
- [4] D. M. Sullivan, *Electromagnetic Simulation Using the FDTD Method* (Institute of Electrical and Electronics Engineers, New York, NY, 2000).
- [5] A. Taflove and S. C. Hagnes, *Computational Electrodynamics: The Finite-Difference Time-Domain Method, 2nd ed.* (Artech House, Norwood, MA, 2000).
- [6] N. Simicevic and D. T. Haynie, *Phys. Med. Biol.*, **50**, 347 (2005).
- [7] N. Simicevic, *Phys. Med. Biol.* **50**, 5041 (2005); *Health Physics. The Radiation Safety Journal* **92**, 574 (2007); *Phys. Med. Biol.* **53**, 1795 (2008);
- [8] J. J. Sakurai, *Advanced Quantum Mechanics* (Addison-Wesley, Redwood City, CA, 1987).
- [9] Z. P. Liao, H. L. Wong, G. P. Yang, and Y. F. Yuan, *Scientia Sinica*, **28**, 1063 (1984).
- [10] K. Huang, *Am. J. Phys.* **20**, 479 (1952).
- [11] D. I. Blohincev, *Prostranstvo i vremya v mikromire* (Nauka, Moscow, 1982).
- [12] N. Simicevic, <http://www.phys.latech.edu/~neven/dirac>
- [13] A. I. Akhiezer and V. B. Beresteckii, *Quantum Electrodynamics* (John Wiley and Sons, New York, 1965).
- [14] V. B. Beresteckii, E. M. Lifshitz, and L. P. Pitaevskii, *Quantum Electrodynamics* (Butterworth Heinemann, Oxford, 1982).